Spectroscopy of the halo nucleus ^{11}Li by an experimental study of ^{11}Li+p collisions

A. A. Korsheninnikov,[1,*] E. Yu. Nikolskii,[2] T. Kobayashi,[1] A. Ozawa,[1] S. Fukuda,[1] E. A. Kuzmin,[2] S. Momota,[1] B. G. Novatskii,[2] A. A. Ogloblin,[2] V. Pribora,[2] I. Tanihata,[1] and K. Yoshida[1]

[1]*RIKEN, 2-1 Hirosawa, Wako, Saitama 351-01, Japan*

[2]*Kurchatov Institute, Kurchatov sq. 1, Moscow 123182, Russia*

(Received 18 September 1995)

An experimental study of ^{11}Li+p collisions at 75A MeV was performed. The excited state of ^{11}Li at $E^*=1.25\pm0.15$ MeV was observed, which is a candidate for a neutron halo excitation. Four other ^{11}Li states were manifested (at $\sim$3.0, 4.9, 6.4, and 11.3 MeV). Angular distributions were measured for elastic scattering ^{11}Li+p and ^{8}He+p. Structure of the ^{11}Li halo was investigated using the eikonal approach.

PACS number(s): 25.60.Gc, 21.45.+v, 23.20.En, 27.20.+n

Nowadays, the neutron rich nucleus ^{11}Li presents one of the most exciting problems in nuclear physics. This nucleus has extraordinary large radius [1] reflecting such an exotic phenomenon as neutron halo [2]. Numerous studies were performed to investigate structure of the ^{11}Li ground state (e.g., see [3–5]). At the same time, the question about the ^{11}Li structure is related to interrogation on its excited states. Corresponding experimental studies are especially important because a new type of excitation, soft dipole mode, is expected to be a consequence of neutron halo. However, reflecting experimental difficulties, the number of spectroscopic studies of ^{11}Li is restricted to two papers only [6,7].

In Ref. [6], the reaction ^{11}B(π^-,π^+)^{11}Li was used to search for excited states of ^{11}Li for the first time, and a weak manifestation of the ^{11}Li state at $E^*=1.2\pm0.1$ MeV was obtained. In Ref. [7], spectroscopy of ^{11}Li was performed using reactions ^{10}Be(^{14}C,^{13}N)^{11}Li and ^{14}C(^{14}C, ^{17}F)^{11}Li. Observation of three excited states of ^{11}Li was reported: at $E^*=2.47\pm0.07$, 4.85 ± 0.07, and 6.22 ± 0.07 MeV. These states were not seen in [6], while the state at 1.2 MeV reported in [6] was not observed in [7]. These circumstances as well as low statistics in [6] and high backgrounds from constituents of complex targets in [7] prompted us to perform a new spectroscopic study of ^{11}Li by means of scattering ^{11}Li+p. The key point of the experiment was correlational measurement of emitted particles.

The *experiment* was carried out in RIKEN (Japan). We used radioactive beam ^{11}Li and studied collisions ^{11}Li+p by the missing mass method detecting recoil protons both in an inclusive way and in coincidence with particles from breakup of ^{11}Li.

The secondary beam was produced by the RIPS facility (Riken projectile-fragment separator) from fragmentation of ^{18}O primary beam at 100A MeV on a ^{9}Be target with thickness 1.1 g/cm^2. The obtained ^{11}Li beam had intensity 2×10^4 pps and energy $E^{\rm lab}=74.5A$ MeV (broadening $\pm3.0A$ MeV).

The experimental setup is shown in Fig. 1. Plastic scintillators and MWPC's were used for projectile identification, tracking, and measurement of ^{11}Li energy. The ^{11}Li beam hit target CH_2 or C with thickness of 11.75 mg/cm^2 or 9.5 mg/cm^2, respectively. All data presented in this paper correspond to the pure proton target (negligible background from C was subtracted).

To detect protons, we used two telescopes of solid state detectors with large area. Every telescope consisted of two strip detectors and three silicon detectors. The centers of telescopes were located at 69°, that is, in the range of small center-of-mass angles in scattering ^{11}Li+p, where cross sections should be higher. The measured energy and angles of every proton allowed us to determine energy in the residual ^{11}Li-like system. Resolution over excitation energy of ^{11}Li (FWHM $\sim$1.5 MeV) was mainly due to the angular resolution of setup and the target thickness.

Charged particles from breakup of ^{11}Li were bent in the magnet and detected by the drift chamber and the plastic scintillators' hodoscope. Neutrons from decay of ^{11}Li were detected by the plastic scintillators' walls. This part of the detection system allowed us to study exclusive spectra of protons in coincidence with Li isotopes and neutrons.

The RIPS facility was tuned to produce a two component secondary beam, which also contained nuclei ^{8}He at 66A MeV ($\pm2A$ MeV), and we studied the ^{8}He+p scattering simultaneously.

To obtain the *resulting spectra* in Fig. 2, we converted the measured distributions $d^2N/dE_p^{\rm lab}d\Omega_p^{\rm lab}$ in $d^2N/dE^*_{^{11}{\rm Li}}d\Omega_p^{\rm lab}$ and integrated them over angular acceptance of proton telescopes ($\theta_p^{\rm lab}\sim60°-80°$).

The inclusive spectrum of protons is shown in Fig. 2(a). A strong peak corresponding to the ^{11}Li ground state is seen. Physical backgrounds are illustrated by curves which clarify the general trend in the high energy part of the spectrum

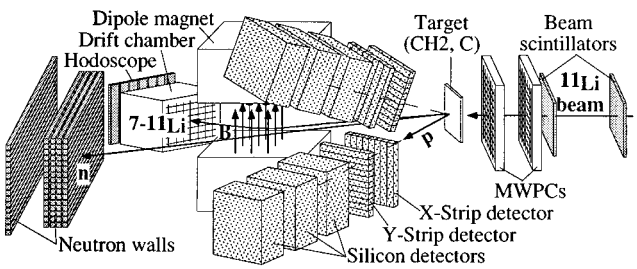

FIG. 1. The experimental setup.

*On leave from Kurchatov Institute, Moscow 123182, Russia.

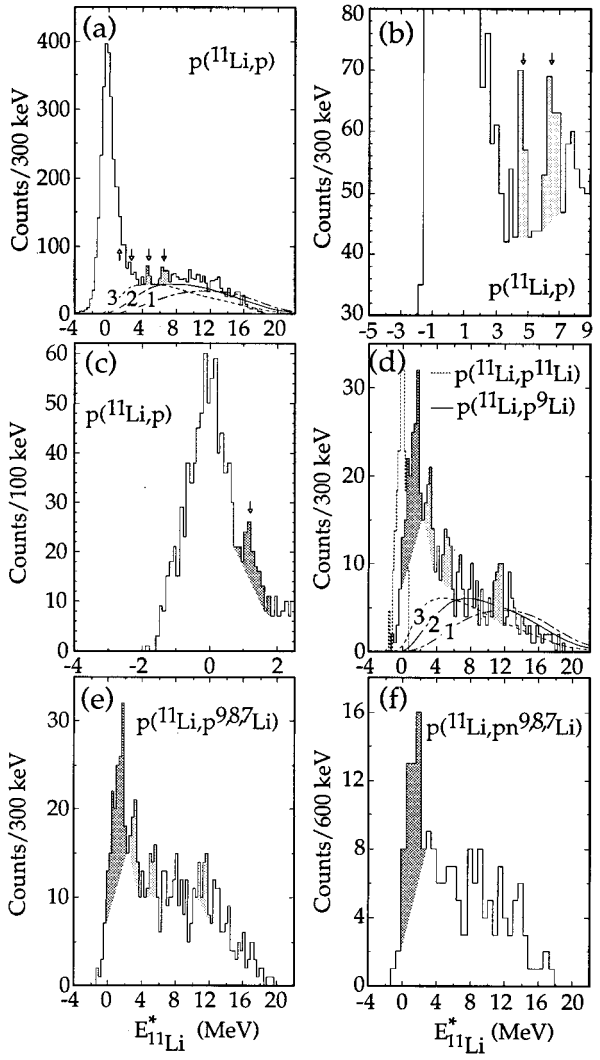

FIG. 2. Proton spectra from the processes indicated on the figure. Arrows mark the ^{11}Li states reported in [6,7]. Curves shows: 1—phase space $p+n+n+{}^9$Li; 2—final state interaction via virtual state ($n+n$ or $n+{}^9$Li); 3—final state interaction via narrow low-energy resonance ^{10}Li.

(detection acceptances and resolutions were taken into account in the calculations). The curve 1 corresponds to a phase space in the channel $p+n+n+{}^9$Li. The curve 2 shows calculation for the $n+n$ final state interaction. Sensitivity to a scattering length is low, and calculations for the $n+{}^9$Li final state interaction via virtual state with parameters providing low energy peak in the system ^{10}Li [8,9] give results similar to the curve 2. The curve 3 presents an extreme case and corresponds to the $n+{}^9$Li final state interaction at the state ^{10}Li, which was considered as a low energy resonance with negligible width (δ function over the n-^{9}Li relative energy; this case can be interpreted as an extreme presentation of resonance with $l=1$ in ^{10}Li).

Arrows in Fig. 2(a) show positions of the ^{11}Li excited states reported in [6,7]. Corresponding to arrows at higher energy, two peculiarities are seen in the experimental data, which are demonstrated in Fig. 2(b) in larger scale. Two arrows at lower energies in Fig. 2(b) are located in the region of tail from the ^{11}Li ground state, showing the necessity to

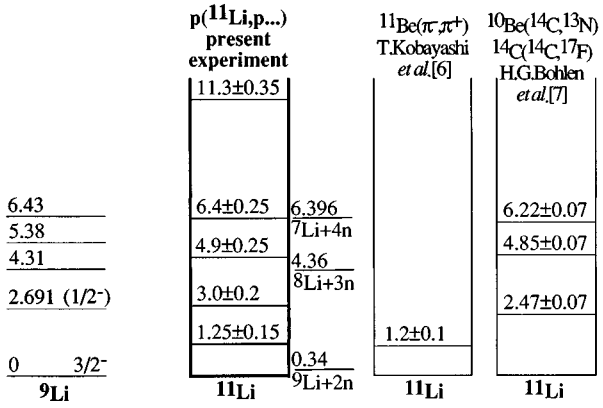

FIG. 3. The obtained data on the ^{11}Li states. Two schemes on the right side show results of [6,7]. The scheme on the left side presents levels of ^{9}Li.

investigate proton spectra in coincidence with particles from decay of ^{11}Li. However, an interesting result can be seen in the inclusive spectrum if we decrease bin size and improve resolution by rejecting events with low energy protons (the resolution is energy dependent reflecting, e.g., the target thickness). Such a spectrum presented in Fig. 2(c) shows a peak in agreement with [6]. This state of ^{11}Li is clearly seen with obvious statistical significance in Fig. 2(d), where the solid histogram presents the proton spectrum detected in coincidence with ^{9}Li. The same state of ^{11}Li at $E^*=1.25\pm0.15$ MeV is observed in Figs. 2(e) and 2(f) also, where we show proton spectra from the processes $p(^{11}\mathrm{Li},p^{9,8,7}\mathrm{Li})$ and $p(^{11}\mathrm{Li},pn^{9,8,7}\mathrm{Li})$, respectively. The observed width of the state is close to the experimental resolution.

In Figs. 2(d) and 2(e), a group on the right side from the 1.25-MeV peak attracts attention. If this is one more excited state of ^{11}Li, it is located at higher energy, $E^*=3.0\pm0.2$ MeV, than the state at $E^*=2.47\pm0.07$ MeV reported in [7], and we suppose that two peaks at $\sim$1.25 and 3.0 MeV were not resolved in [7]. One more tentative group might be distinguished in Fig. 2(d) at $E^*=4.9\pm0.25$ MeV. At last, note a structure at 11.3 ± 0.35 MeV in Fig. 2(d). The corresponding peak is seen in the spectrum from reaction ^{14}C(^{14}C, ^{17}F)^{11}Li [7].

Finally, the peak at 1.25 MeV is statistically convincing. The smaller hatched peaks in Fig. 2 are less convincing,[1] but together with the results of [7] the assignments of the corresponding states of ^{11}Li seem plausible. All obtained data about the ^{11}Li states are summarized in Fig. 3. Let us comment on the possible nature of these levels. (I) The first excited state of ^{11}Li probably corresponds to an excitation of

[1]For example, two peaks in Fig. 2(b) might be interpreted as statistically significant, but the peak at $E^*\sim4.9$ MeV seems to be too narrow (at the same time, in combination with low background, this peak can be reproduced within statistically allowed limits by Gaussian with reasonable width) while the peak at $\sim$6.4 MeV is separated from the right-side structure by one channel only. In addition, whereas the coincidence spectra show a structure at $\sim$4.9 MeV, they do not confirm a peak at $\sim$6.4 MeV.

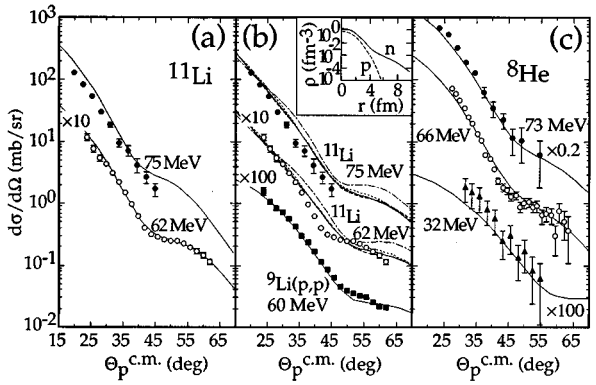

FIG. 4. (a) Angular distributions for elastic scattering ^{11}Li$+p$ at 75A MeV (present experiment) and 62A MeV [11]. Curves show optical model calculations (see the text). (b) Angular distributions for ^{11}Li$+p$ at 75A and 62A MeV and ^{9}Li$+p$ at 60A MeV [11]. Curves show eikonal calculations (see the text). Inset illustrates the $n(p)$ densities in ^{11}Li. (c) Angular distributions for elastic scattering ^{8}He$+p$ at 66A MeV (present experiment), 73A MeV [12], and 32A MeV [13]. Curves present the eikonal calculations.

halo neutrons. Apart from an assumption that this is the soft dipole mode excitation [6], there is another possibility: the state suggested in [10] with the same quantum numbers $J^\pi=3/2^-$ as that for the ground state. (II) The excitation energy of the second state of ^{11}Li is close to that of the first excited state of ^{9}Li, and this state of ^{11}Li at $\sim$3.0 MeV might have the excited ^{9}Li core and the corresponding $J^\pi=(1/2^-)$ of the ^{9}Li excited state (Fig. 3). (III) If we sum energies of two lowest states in ^{11}Li, the result is similar to the energy of the third excited state of ^{11}Li, which might have both the excited ^{9}Li core and the valence neutron excitation. (IV) Excitation energy of the fourth excited state of ^{11}Li is very close to the energy of the ^{9}Li state at 6.43 MeV, which is located in the vicinity of threshold ^{7}Li$+n+n$ and should have component with spatially extended two-neutrons. Two extra neutrons in ^{11}Li allow to assume a structure "^{7}Li-core+4-neutron halo" for the ^{11}Li state at $\sim$6.4 MeV. This state is really located in close vicinity of 4-neutron threshold, which might provide spatial extension of wave function.

The measured *angular distribution* for the ^{11}Li$+p$ elastic scattering at 75A MeV is shown in Fig. 4(a), where the data obtained at 62A MeV [11] are presented also. Curves correspond to the optical model calculations for these two energies with parameters fitted to the data at 62A MeV (potential B in [11]). The calculation reproduces the result of the present experiment rather well, showing that the data measured at two energies are satisfactorily consistent in the overlapping angular range. Some overestimation for the curve at 75A MeV can be attributed to an energy dependence of potential.

In Ref. [14], the optical model was used to analyze the angular distribution at 62A MeV as well as the data for scattering ^{9}Li$+p$ [11]. The latter is presented on the bottom of Fig. 4(b), which shows the ^{11}Li$+p$ data also. A similarity between shapes of the ^{11}Li$+p$ and ^{9}Li$+p$ data was interpreted in [14] as a consequence of ^{11}Li structure "^{9}Li-core plus low-density neutron halo."

Elastic scattering data are often expected to provide new information about the halo structure. We study this problem considering four extreme assumptions about valence neutrons' configurations in ^{11}Li and analyze the experimental data using the eikonal approach which contains no fitting parameters.

The amplitude for an elastic proton scattering is given by [15]:

$$f=ik\int J_0(e^{i\chi_C}-e^{i\chi_C+i\chi_N})b\ db+f_C, \tag{1}$$

where $f_C(\theta)$ and χ_C are standard Coulomb amplitude and phase taken for a uniform charged sphere with $R_C=r_{0C}A^{1/3}$ ($r_{0C}=1.33$ fm for ^{9}Li and 1.1 fm for ^{4}He [16]). The nuclear phase χ_N is determined by optical potential V_N in the $t\rho$ approximation [15]:

$$\chi_N(b)=-\frac{1}{\hbar v}\int dz\ V_N(\sqrt{b^2+z^2}), \tag{2}$$

$$V_N=\bar{t}_{pn}\rho_n+\bar{t}_{pp}\rho_p,\quad \bar{t}_{pN}=-\frac{\hbar v}{2}\bar{\sigma}_{pN}(\alpha_{pN}+i). \tag{3}$$

In Eq. (3), $\rho_{p(n)}$ is proton (neutron) density of nucleus. The Pauli-corrected pN total cross section, $\bar{\sigma}_{pN}=\sigma_{pN}P(\varepsilon_{NF}/\varepsilon)$ [17], depends on the Fermi energy of target nucleon, ε_{NF}, calculated for $\rho_{p(n)}$. The energy ε of incident proton at the interaction point was evaluated using the Coulomb potential and the real part of V_N. In addition to $\rho_{p(n)}$, input for calculations includes parameters of the pN amplitude, σ_{pN} and α_{pN}. The total cross sections σ_{pN} are known in the energy range under consideration, $E\leqslant 100$ MeV (e.g., [18]); we approximated them by $\sigma_{pp}[\mathrm{mb}]=1/(-1.4\times10^{-3}+4.45\times10^{-4}E-7.37\times10^{-7}E^2)$ and $\sigma_{pn}[\mathrm{mb}]=1/(-2.5\times10^{-4}+1.15\times10^{-4}E+1.73\times10^{-7}E^2)$ (E in MeV). Parameters α_{pN} are known at $E\geqslant 100$ MeV. We used interpolations, $\alpha_{pp}=2.55-6.8\times10^{-3}E$ and $\alpha_{pn}=1.08-8.0\times10^{-4}E$, from the values of α_{pN} [19] at two lowest energies.

The result of the calculation for scattering ^{9}Li$+p$ is shown in Fig. 4(b) for the Gaussian proton and neutron densities with the same radii, $R^{\mathrm{exp}}_{\mathrm{mat}}(^{9}\mathrm{Li})=2.32$ fm [1]. We also tried the shell-model densities [20] with nonidentical shapes for protons and neutrons; the result is close to the curve in Fig. 4(b). As it is seen in the figure, the calculation reasonably describes the experimental data. We shall use this approach to compare results obtained in different assumptions on the ^{11}Li halo.

The ^{11}Li densities were obtained in the ^{9}Li$+n+n$ model using the cluster-orbital shell-model approximation (COSMA) [5]. For the ^{9}Li core we used the Gaussian proton and neutron densities [$R^p_{\mathrm{rms}}=R^n_{\mathrm{rms}}=R^{\mathrm{exp}}_{\mathrm{mat}}$ (^{9}Li)]. The halo density was taken for four extreme cases: two valence neutrons are in $1p$, $2s$, $1d$, and $1s$ state [5]:

$$\rho^{1p}=2\times3^{-1}\pi^{-1.5}\alpha^{-3}x^2e^{-x^2}, \tag{4}$$

$$\rho^{2s}=2\times3^{-1}\pi^{-1.5}\alpha^{-3}(x^2-1.5)^2e^{-x^2}, \tag{5}$$

$$\rho^{1d}=4\times15^{-1}\pi^{-1.5}\alpha^{-3}x^4e^{-x^2}, \tag{6}$$

$$\rho^{1s} = \pi^{-1.5}\alpha^{-3}e^{-x^2} \tag{7}$$

(the $1s$ state for the halo neutrons is not straightforwardly forbidden in COSMA [5]). In Eqs. (4)–(7), $x = r/\alpha$ and the scale parameter α corresponds to the experimental radius of ^{11}Li, $R_{\rm mat}^{\rm exp}(^{11}{\rm Li}) = 3.2$ fm [1] ($\alpha_{1p} = 3.78$ fm, $\alpha_{2s} = \alpha_{1d} = 3.2$ fm, $\alpha_{1s} = 4.88$ fm [5]). The inset in Fig. 4(b) shows neutron and proton densities on an example of the $1p$ case.

Calculated cross sections for scattering $^{11}{\rm Li} + p$ at two energies are presented in Fig. 4(b) by solid, dotted, dashed, and dash-dotted curves corresponding to the halo neutrons in the $1p$, $1s$, $1d$, and $2s$ state, respectively. The results are in satisfactory agreement with the experimental data. The curves for $1l$ states are very close to each other. The dash-dotted curve ($2s$) deviates from other results, but difference of such a scale would be meaningful only after appearance of high precision theory for elastic scattering. The curves in Fig. 4(b) correspond to the extreme cases with pure states. The performed calculations for more realistic mixtures [5] between these configurations gave results indistinguishable from the group of $1l$ curves in Fig. 4(b). Thus, angular distributions (at least at low energies) seem not to be a very promising tool to study details of halo structure. (For a sensitivity to such a gross characteristic of halo as a matter radius, see [21].)

In Fig. 4(c), the measured angular distribution for elastic scattering $^{8}{\rm He} + p$ at 66A MeV is shown by black circles; other angular distributions at 73A and 32A MeV were measured previously [12,13]. Curves, which show the above described eikonal calculations with the COSMA densities obtained in the $\alpha + 4n$ model for ^{8}He [22], are in a reasonable agreement with the experimental data.

Summarizing, we have studied collisions $^{11}{\rm Li} + p$ at 75A MeV by correlational measurements. The proton spectra definitely show the low-energy excited state of ^{11}Li at $E^* = 1.25 \pm 0.15$ MeV. Comparison with the excited states of ^{9}Li suggests that this state of ^{11}Li corresponds to the halo excitation. In addition, the following ^{11}Li states were manifested: at $E^* = 3.0 \pm 0.2$, 4.9 ± 0.25, 6.4 ± 0.25, and 11.3 ± 0.35 MeV (Fig. 3). Angular distributions were measured for elastic scattering $^{11}{\rm Li} + p$ at 75A MeV and $^{8}{\rm He} + p$ at 66A MeV.

The existing data for elastic scattering $^{11}{\rm Li} + p$ and $^{8}{\rm He} + p$ were analyzed in the parameter-free eikonal approach and a reasonable description of the experimental data was found. A sensitivity to the valence neutrons' configurations in ^{11}Li was investigated and it was demonstrated that an elastic scattering at low energies seems not to be a very promising tool to study details of halos.

This work was supported in part by Grant-in-Aid for Scientific Research on Priority Areas (No. 05243102) from the Ministry of Education, Science and Culture.

[1] I. Tanihata *et al.*, Phys. Rev. Lett. **55**, 2676 (1985).
[2] P. G. Hansen and B. Jonson, Europhys. Lett. **4**, 409 (1987).
[3] I. Tanihata, Prog. Part. Nucl. Phys. **35**, 505 (1995).
[4] K. Riisager, Rev. Mod. Phys. **66**, 1105 (1994).
[5] M. V. Zhukov *et al.*, Phys. Rep. **231**, 151 (1993).
[6] T. Kobayashi, Nucl. Phys. **A538**, 343c (1992).
[7] H. G. Bohlen *et al.*, Z. Phys. A **351**, 7 (1995).
[8] A. I. Amelin *et al.*, Sov. J. Nucl. Phys. **52**, 782 (1990).
[9] R. A. Kryger *et al.*, Phys. Rev. C **47**, R2439 (1993).
[10] I. J. Thompson and M. V. Zhukov, Phys. Rev. C **49**, 1904 (1994).
[11] C.-B. Moon *et al.*, Phys. Lett. B **297**, 39 (1992).
[12] A. A. Korsheninnikov *et al.*, Phys. Lett. B **316**, 38 (1993).
[13] A. A. Korsheninnikov *et al.*, Phys. Lett. B **343**, 53 (1995).
[14] S. Hirenzaki *et al.*, Nucl. Phys. **A552**, 57 (1993).
[15] C. A. Bertulani *et al.*, Phys. Rep. **226**, 281 (1993).
[16] C. M. Perey *et al.*, Nucl. Data Tables **10**, 539 (1972).
[17] E. Clementel and C. Villi, Nuovo Cimento **II**, 176 (1955).
[18] W. O. Lock and D. F. Measday, *Intermediate Energy Nuclear Physics* (Menthuen, London, 1970).
[19] L. Ray, Phys. Rev. C **20**, 1857 (1979).
[20] G. F. Bertsch *et al.*, Phys. Rev. C **39**, 1154 (1989).
[21] L. V. Chulkov *et al.*, Nucl. Phys. **A587**, 291 (1995).
[22] M. V. Zhukov *et al.*, Phys. Rev. C **50**, R1 (1994).